Journal of Diabetes Science and Technology
2021, Vol. 15(4) 781–785

DOI: 10.1177/1932296820920948
journals.sagepub.com/home/dst


Safety and Functional Integrity of Continuous Glucose Monitoring Components After Simulated Radiologic Procedures

Christopher Thomas, MEng, John B. Welsh, MD, PhD, Spencer Lu, BS, and J. Michael Gray, MS

Abstract

Background: We investigated wearable components of the Dexcom G6 continuous glucose monitoring (CGM) System in simulated therapeutic and diagnostic radiologic procedures.

Methods: G6 transmitters were loaded with simulated glucose data and attached to sensors. Sets of sensor/transmitter pairs were exposed to x-rays to simulate a radiotherapeutic procedure and to radiofrequency (RF) and magnetic fields to simulate diagnostic magnetic resonance imaging (MRI). The x-ray simulation provided a cumulative dose of 80 Gy. The MRI simulation used RF fields oscillating at 64 or 128 MHz and magnetic fields of 1.5 or 3 T. During the MRI simulation, displacement force, induced heating, and induced currents were measured. After the simulations, bench tests were used to assess data integrity on the transmitters and responsiveness of sensors to various concentrations of aqueous glucose.

Results: Glucose concentrations reported by sensor/transmitter pairs after undergoing x-irradiation or a simulated MRI exam were similar to those from control (unexposed) devices. During the 3 T MRI simulation, the devices experienced a displacement force of 306 g, which was insufficient to dislodge the sensor/transmitter from the substrate, RF-induced heating of <2°C, and an induced current of <16 pA. Data stored on the transmitters prior to the MRI simulation remained intact.

Conclusion: Wearable components of the G6 CGM System retain basic functionality and data integrity after exposure to simulated therapeutic and diagnostic radiologic procedures. The devices are unlikely to be affected by x-irradiation used in typical imaging studies. Simulated MRI procedures create displacement force, minimal heating, and current in sensor/transmitter pairs.

Keywords

continuous glucose monitoring, G6, imaging, MRI, radiation, x-rays

Introduction

Continuous glucose monitoring (CGM) systems are increasingly prevalent tools in diabetes management[1]; the data they provide can inform treatment decisions[2] and, in some instances, can govern insulin delivery.[3] The Dexcom G6 CGM System (Dexcom, Inc., San Diego, CA) includes two body-worn components: a single-use, subcutaneously worn sensor wire that is inserted with the aid of a specialized applicator and a multiuse, externally worn transmitter. The non-ferromagnetic sensor wire serves to immobilize electrochemically active glucose oxidase and is part of a larger sensor unit, which includes a skin-facing adhesive patch and a bracket for securely attaching a transmitter. The transmitter houses a battery, along with circuitry for signal processing, data storage, and Bluetooth low energy (BLE) connectivity. Although sensor units can be easily removed from the skin and transmitters can be easily removed from the sensor units, a removed sensor wire cannot be reinserted and once a transmitter is removed from the bracket, it cannot be reattached.

Currently, G6 users are given specific instructions for airport security checkpoints, including to avoid going through whole-body millimeter wave scanners and to avoid putting any G6 components through baggage x-ray machines.[4] Wearable G6 components are labeled as "MR Unsafe" and

Dexcom Inc., San Diego, CA, USA

Corresponding Author:
John B. Welsh, MD, PhD, Dexcom Inc., 6340 Sequence Drive, San Diego, CA 92121, USA.
Email: john.welsh@dexcom.com

are contraindicated for magnetic resonance imaging (MRI), computed tomography (CT), and diathermy. Wearable G6 components have not been extensively studied in the clinical setting under electromagnetic fields and ionizing radiation conditions. It is possible that electromagnetic fields, heat, and/or ionizing radiation could damage G6 components, leading to inaccurate glucose values or missed alerts. It is also possible that devices heated or displaced by magnetic fields could injure patients.

To assess whether body-worn G6 components maintain their stored data and basic functional integrity after simulated radiologic procedures, we exposed sensors and transmitters to a high cumulative dose of x-rays (to simulate radiotherapy) and to oscillating radiofrequency (RF) electromagnetic fields combined with strong magnetic fields (to simulate MRI exams). Cumulative doses of x-rays are expressed in gray (Gy), where 1 Gy = 1 joule absorbed per kilogram of matter. The energy of individual x-rays is given in MeV (megaelectron volts). Magnetic flux density is measured in teslas (T), where 1 T = 1 volt·second per meter squared.

Methods

X-Irradiation

To evaluate the response of wearable G6 components to therapeutic x-rays, independent sensors and sensor units attached to transmitters were exposed to 6 MeV photons from a particle accelerator at the highest rate used in radiotherapy for a cumulative dose of 80 Gy. The devices were new at the time of testing, and the sensor wires were neither hydrated nor exposed to glucose. After irradiation, Dexcom internal feasibility protocols were executed to investigate G6 functionality. Bench testing on 48 exposed and 48 nonexposed G6 sensors was performed over several days across the functional range of glucose concentrations, to evaluate the impact of high-dose radiation on sensor responsiveness to glucose over time. Twenty G6 transmitter and sensor pairs were connected to receiving devices via BLE several times over 10 days following radiation to evaluate for a loss of BLE functionality over a new wear period.

Magnetic Resonance Imaging

In silico modeling was conducted before MRI exposure to determine the position and orientation of the hardware that was likely to encounter the highest heating. Physical testing of the G6 was then performed according to the ASTM F2182 standard[5] at the identified location and orientation. Temperature was measured at four-second intervals using a Luxtron Model 3100 Fluoroptic Thermometry System, with a temperature resolution of 0.1°C and spatial resolution of <1 mm. Peak displacement force was measured with a digital force gauge in a 3 T static magnetic field. The device was attached via a string to a digital force gauge positioned 9 feet from the MR system to avoid magnetic influence. The force gauge was moved toward the G6 sensor to remove tension and then moved away to establish the maximum translational force as described previously.[6,7] Afterward, the G6 was attached to an imaging phantom by its adhesive patch and positioned at the point of highest spatial gradient to test whether the magnetic force alone could dislodge it.

To evaluate the response of G6 components to MRI conditions, 48 new G6 sensor/transmitter units were placed inside the coil of an MRI, half in a 3 T system and the other half in a 1.5 T system. The sensors were neither hydrated nor exposed to glucose during the simulation. The devices were imaged across a range of settings and orientations that had been used elsewhere[8] to evaluate edge-case imaging conditions for a different implantable medical device. Total time inside the energized MRI coil was ~45 minutes. A control group of sensor/transmitter pairs was kept outside the coil, with the sensors similarly dry and unexposed to glucose. Dexcom internal feasibility protocols were executed to investigate the functionality of G6 transmitter and sensor. Twelve of the transmitters had been previously loaded with simulated glucose values prior to exposure with the data downloaded after exposure and compared against loaded data to evaluate for loss or corruption. Bench tests on 24 exposed and six nonexposed G6 devices were performed using device functional range of glucose concentrations to evaluate impact to glucose performance following MRI exposure. Twelve G6 devices were recording a background signal (without the sensors being exposed to glucose) during the MRI exposure to observe if field effects were detected by the transmitter/sensor and recorded values were downloaded. All 48 test G6 transmitter and sensor pairs were connected to via BLE several times for 14 days after MRI to evaluate for a loss of BLE functionality over a new wear period.

Results

Effect of X-irradiation on Measured Glucose Concentrations and Coefficients of Variation

The 96 Dexcom G6 sensors underwent bench testing after irradiation alongside control sensors to evaluate response to aqueous glucose concentrations of 40, 160, 280, and 400 mg/dL. This testing was performed immediately upon return from the radiation test facility and performed repeatedly over 21 days. Approximately 10 glucose readings were obtained at every step to produce a mean glucose reading for each sensor at each glucose concentration. Table 1 shows the differences in mean glucose concentrations between the nonirradiated and irradiated sensors, normalized for glucose concentration. The difference in mean glucose between irradiated and control units was typically <1 mg/dL, and no trends were apparent. Coefficients of variation for sensors that were or were not irradiated are shown in Table 2. Although higher among irradiated sensors, coefficients of variation were low (typically <1%) for both groups of sensors, and were highest at the lowest glucose concentrations.

Table 1. Differences in Mean Glucose Concentrations Measured by Sensors that were Nonirradiated and Irradiated at Various Times and Glucose Concentrations.

	Aqueous glucose concentration (mg/dL)			
Time and sample size	40	160	280	400
Before radiation testing $N_1 = 47$; $N_2 = 48$	0.11	0.03	–0.37	0.24
Day 0 $N_1 = 46$; $N_2 = 45$	–0.43	0.68	–0.06	–0.19
Day 10 $N_1 = 44$; $N_2 = 47$	0.1	–0.2	0.09	0.01
Day 14 $N_1 = 46$; $N_2 = 46$	0.39	0.62	–2.44	1.42
Day 21 $N_1 = 48$; $N_2 = 40$	0.14	–0.11	–0.18	0.16

Values are calculated as (nonirradiated mean – irradiated mean), divided by the nominal ambient glucose concentration. The number of sensors in each day's nonirradiated group and irradiated group is given as N_1 and N_2, respectively.

Table 2. Coefficients of Variation of Mean Glucose Concentrations Reported by Nonirradiated and Irradiated Sensors at Various Times and Glucose Concentrations.

			Aqueous glucose concentration (mg/dL)			
Sensor group	Time	*N*	40	160	280	400
Nonirradiated	Before radiation testing	47	1.41	0.39	0.34	0.19
	Day 0	46	0.54	0.25	0.20	0.08
	Day 10	44	0.70	0.19	0.18	0.09
	Day 14	46	1.85	1.01	1.44	0.56
	Day 21	48	2.00	0.82	0.30	0.16
Irradiated	Before radiation testing	48	0.62	0.24	0.16	0.08
	Day 0	45	2.26	0.97	0.12	0.12
	Day 10	47	1.11	0.36	0.16	0.10
	Day 14	46	2.37	1.10	2.04	0.83
	Day 21	40	3.62	1.38	0.32	0.26

Post-X-Ray BLE Functionality

Following irradiation, all 20 G6 devices were sent through multiple BLE connection cycles with a receiving device over a period of 10 days. Each device underwent from 10 to 15 connection cycles, with no failed connection attempts.

MRI Heating Simulation and Testing

In silico modeling of expected heating of G6 components in various positions and orientations suggested a worst-case scenario for testing of the components attached to a phantom. Exposure of the components to a 3 T/128 MHz simulated MRI exam showed differential heating of adjacent and nonadjacent temperature probes (Figure 1). Probe 1 was adjacent to body-worn G6 components and experienced a maximum temperature change of +1.6°C; probe 2 was not adjacent and experienced a maximum temperature change of +0.7°C.

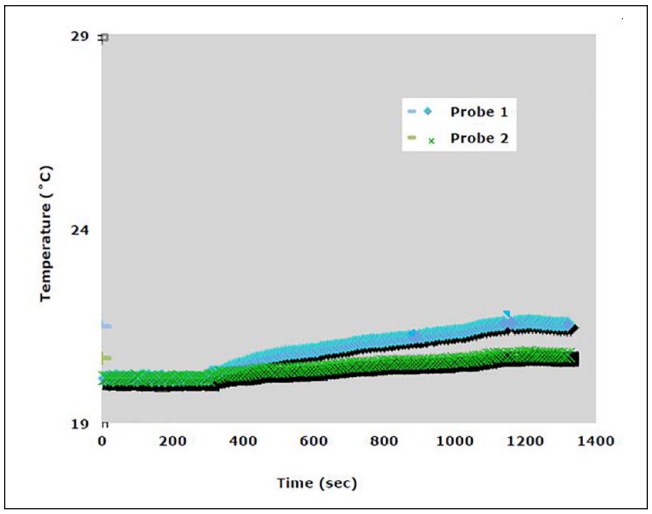

Figure 1. Temperature change recorded by probes exposed to a 20-minute, 3 T/128 MHz simulated MRI exam. Probe 1 was adjacent to body-worn components of the G6 CGM System; Probe 2 was nonadjacent. MRI, magnetic resonance imaging.

MRI Displacement Force

Peak displacement force on the G6 device under a static 3 T field was 306 g (0.68 lb). The sensor unit's adhesive patch was sufficient to maintain attachment to an imaging phantom when exposed to this force (not shown).

Data Integrity Post-MRI

The stored 10 days of glucose values were downloaded from each of the 12 transmitters and evaluated against the source information. The glucose data matched the simulated data identically for every device following both 1.5 and 3 T exposures; there was no data loss or corruption.

Data Accumulation During MRI Exposure

Data collected from the six 1.5 T-exposed and six 3 T-exposed G6 devices allowed observation of background currents generated during the exposures. All devices showed a spike in current shortly after entering the MRI. Figure 2 shows an example of the current generated by 3 T/128 MHz MRI; the response to a 1.5 T/64 MHz MRI was effectively equivalent (not shown). A similar peak was observed on all devices, though the magnitude varied. After the spike, the current returned to typical levels but continued to fluctuate until

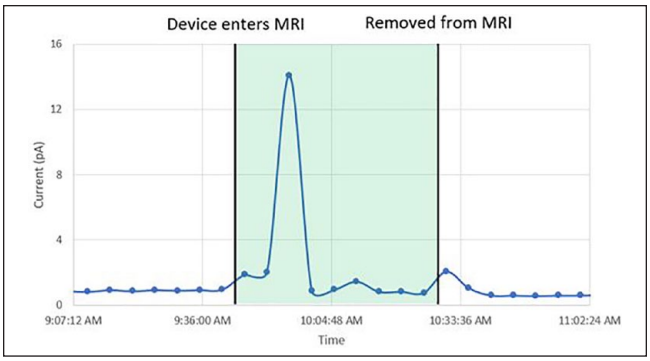

Figure 2. Effect of MRI exposure on background signal accumulation. Shown are data accumulated by a randomly selected single sensor/transmitter pair before, during, and after a 45-minute exposure to eight different scanning sequences in a 3 T magnetic field. MRI, magnetic resonance imaging.

removal. None of the devices experienced an interruption in data recording during or after the exposure.

Post-MRI Performance

The 24 devices exposed to either 1.5 T ($n = 12$) or 3 T ($n = 12$) magnetic fields, along with six control devices that were not exposed to MRI-generated magnetic fields, underwent bench testing to evaluate device response to aqueous glucose concentrations that increased in a stepwise manner from 40 to 400 mg/dL. Approximately five glucose readings were recorded at every glucose concentration. Figure 3 shows currents from a single randomly selected sensor from each of the three groups. Table 3 shows the difference in mean glucose concentrations between control sensors and sensors exposed to either 1.5 or 3 T magnetic fields, normalized for the nominal ambient glucose concentration. The difference in mean glucose between MRI-exposed and control units was typically <1.5 mg/dL and was highest at the lowest glucose concentration. Table 4 shows the coefficients of variation for each of the three groups, which were $<1\%$ at all glucose concentrations except the lowest.

Post-MRI BLE Functionality

All 48 MRI exposed G6 devices successfully connected and communicated via BLE several times over a period of 14 days. No communication abnormalities were observed in any of the devices.

Discussion and Conclusions

Implanted medical devices are a concern in diagnostic and therapeutic radiology. Radiological procedures may alter devices' structure or function during or after an examination, compromising patient safety; conversely, the presence of an implanted device may degrade image quality or complicate efforts to target a particular tumor.

Data presented here suggest that the wearable components of the G6 CGM System maintain their stored data and basic aspects of their functional integrity after exposure to simulated radiologic procedures. The x-ray study used dosing rates and total doses similar to the highest used in treatment of a malignancy, which are far in excess of rates and doses used in CT imaging and conventional (plain) x-ray imaging. Sensors exposed ex vivo to these x-rays behaved similarly to unexposed sensors with respect to their glucose responsiveness. The MRI simulation study revealed that the transmitters' data storage and communications functions remained intact. The magnitude of heating during the 20-minute MRI simulation was <2°C, which is unlikely to cause thermal injury,[9] and the magnitude of the displacement force was insufficient to dislodge the sensor and transmitter from an imaging phantom. However, the devices are MR unsafe and are contraindicated for use during MRI procedures. Users should follow the manufacturer's instructions[4] and should not wear G6 sensors or transmitters during MRI procedures.

Strengths of the study include its use of cumulative doses of high-energy x-rays that are comparable to those used in radiation oncology, and its use of industry-standard methods for determining the safety of devices exposed to the magnetic and oscillating RF fields used in MRI studies. A principal limitation of the study is that none of the exposures or functional tests were conducted in vivo, and functionality of the devices during the exposures was not assessed. In particular, the transmitters were not tested for their ability to communicate during exposure to high-energy x-rays or while inside an energized MRI coil, and the sensors were not exposed to glucose during the simulated MRI exam. Because enzymes such as glucose oxidase are generally more stable when not hydrated or in solution, the performance of sensors exposed to radiologic procedures during their working lives may be different from sensors that are exposed ex vivo. No attempt was made to determine the effect of the interventions to the expected three-month working life of the transmitter. Although glucose values that were stored on G6 transmitters remained intact following MRI exposure, other aspects of G6 transmitter functionality or memory were not evaluated. No testing was performed to determine if transient current spikes observed during MRI exposure would be detected by the system as a sensor failure. The lack of predefined statistical endpoints for functional integrity is another limitation of this study.

Because of the increasing prevalence of CGM systems among patients who may undergo diagnostic and therapeutic radiological procedures, data presented here are informative to healthcare professionals involved in their care, to workers with occupation-related exposure to electromagnetic fields and ionizing radiation who use CGM to help manage their own diabetes, to CGM users undergoing airport screening procedures, and to global regulators.

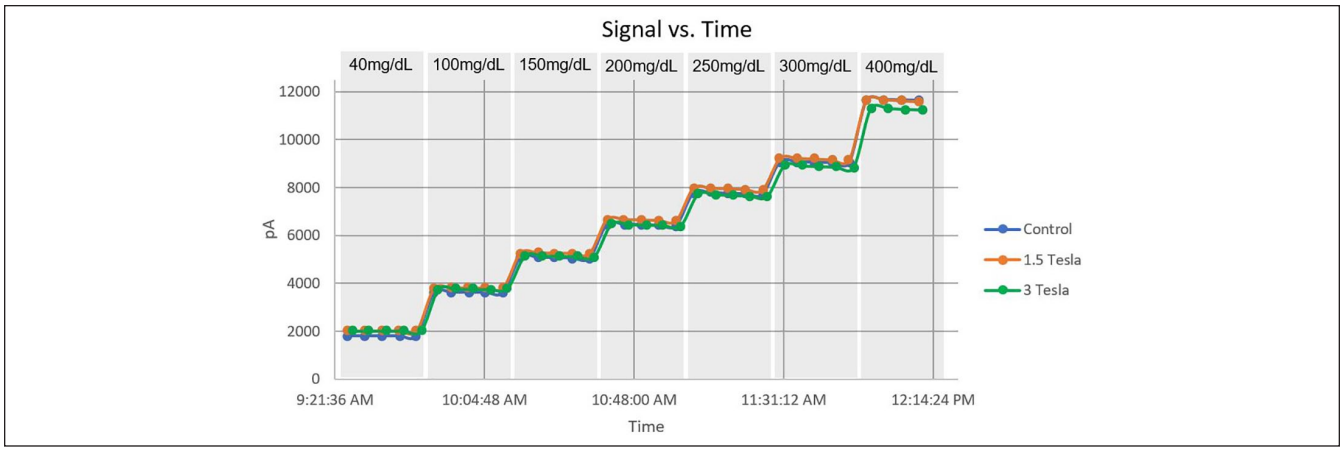

Figure 3. Mean currents (in picoamperes) generated by G6 sensors in response to exposure to stepwise increasing glucose concentrations ranging from 40 to 400 mg/dL. Blue, control sensor with no MRI exposure; orange, sensor exposed to a 1.5 T magnetic field; green, sensor exposed to a 3 T magnetic field. Each curve represents one randomly selected sensor. MRI, magnetic resonance imaging.

Table 3. Differences in Mean Glucose Concentrations Measured by Sensors that were Nonexposed and Exposed to Magnetic Fields at Various Glucose Concentrations.

Magnetic field strength and sample size	Aqueous glucose concentration (mg/dL)						
	40	100	150	200	250	300	400
1.5 T $N_1 = 6$; $N_2 = 12$	2.02	0.65	–0.13	–1.08	–1.23	–0.68	–0.02
3 T $N_1 = 6$; $N_2 = 12$	2.28	0.61	–0.48	–1.24	–1.42	–0.68	0.29

Values are calculated as (nonexposed mean – exposed mean), divided by the nominal ambient glucose concentration. The number of sensors in the nonexposed group and the exposed group is given as N_1 and N_2, respectively.

Table 4. Coefficients of Variation of Mean Glucose Concentrations Reported by Sensors that were not Exposed to MRI-Generated Magnetic Fields (Control) or to 1.5 or 3 T Magnetic Fields at Various Glucose Concentrations.

Magnetic field strength (T)	N	Aqueous glucose concentration (mg/dL)						
		40	100	150	200	250	300	400
0 (control)	6	2.77	0.36	0.48	0.45	0.46	0.33	0.20
1.5	12	4.50	0.59	0.70	0.79	0.71	0.60	0.49
3	12	6.15	0.67	0.43	0.69	0.67	0.49	0.33

Abbreviation: MRI, magnetic resonance imaging.

Declaration of Conflicting Interests

The author(s) declared the following potential conflicts of interest with respect to the research, authorship, and/or publication of this article: The authors are employees of Dexcom, Inc.

Funding

The author(s) disclosed receipt of the following financial support for the research, authorship, and/or publication of this article: Dexcom, Inc.

ORCID iD

John B. Welsh https://orcid.org/0000-0001-9243-5228

References

1. Foster NC, Beck RW, Miller KM, et al. State of type 1 diabetes management and outcomes from the T1D exchange in 2016-2018. *Diabetes Technol Ther*. 2019;21(2):66-72.
2. Pettus J, Edelman SV. Recommendations for using real-time continuous glucose monitoring (rtCGM) data for insulin adjustments in type 1 diabetes. *J Diabetes Sci Technol*. 2017;11(1):138-147.
3. Brown SA, Kovatchev BP, Raghinaru D, et al. Six-month randomized, multicenter trial of closed-loop control in type 1 diabetes. *N Engl J Med*. 2019;381(18):1707-1717.
4. Dexcom. *Dexcom G6 Mobile Continuous Glucose Monitoring System User Guide*. LBL014003 Rev 010 MT23976. San Diego, CA: Dexcom, Inc.; 2018. https://s3-us-west-2.amazonaws.com/dexcompdf/G6-CGM-Users-Guide.pdf. Accessed March 27, 2020.
5. ASTM International. *ASTM. F2182-19e1, Standard Test Method for Measurement of Radio Frequency Induced Heating On or Near Passive Implants During Magnetic Resonance Imaging*. West Conshohocken, PA: ASTM International; 2019.
6. Baker KB, Nyenhuis JA, Hrdlicka G, Rezai AR, Tkach JA, Shellock FG. Neurostimulation systems: assessment of magnetic field interactions associated with 1.5- and 3-Tesla MR systems. *J Magn Reson Imaging*. 2005;21(1):72-77.
7. Shellock FG, Fischer L, Fieno DS. Cardiac pacemakers and implantable cardioverter defibrillators: in vitro magnetic resonance imaging evaluation at 1.5-tesla. *J Cardiovasc Magn Reson*. 2007;9(1):21-31.
8. Weiland JD, Faraji B, Greenberg RJ, Humayun MS, Shellock FG. Assessment of MRI issues for the Argus II retinal prosthesis. *Magn Reson Imaging*. 2012;30(3):382-389.
9. Goldstein LS, Dewhirst MW, Repacholi M, Kheifets L. Summary, conclusions and recommendations: adverse temperature levels in the human body. *Int J Hyperthermia*. 2003;19(3):373-384.